

Investigating the role of the experimental protocol in phenylhydrazine-induced anemia on mice recovery

O. Angulo, Olivier Gandrillon, Fabien Crauste

► **To cite this version:**

O. Angulo, Olivier Gandrillon, Fabien Crauste. Investigating the role of the experimental protocol in phenylhydrazine-induced anemia on mice recovery. *Journal of Theoretical Biology*, Elsevier, 2018, 437, pp.286 - 298. <10.1016/j.jtbi.2017.10.031>. <hal-01646792>

HAL Id: hal-01646792

<https://hal.inria.fr/hal-01646792>

Submitted on 1 Dec 2017

HAL is a multi-disciplinary open access archive for the deposit and dissemination of scientific research documents, whether they are published or not. The documents may come from teaching and research institutions in France or abroad, or from public or private research centers.

L'archive ouverte pluridisciplinaire **HAL**, est destinée au dépôt et à la diffusion de documents scientifiques de niveau recherche, publiés ou non, émanant des établissements d'enseignement et de recherche français ou étrangers, des laboratoires publics ou privés.

Investigating the role of the experimental protocol in phenylhydrazine-induced anemia on mice recovery

O. Angulo^a, O. Gandrillon^{b,d}, F. Crauste^{c,d,*}

^a*Departamento de Matemática Aplicada, ETSIT, Universidad de Valladolid, Pso. Belén 15, 47011 Valladolid, Spain*

^b*Univ Lyon, ENS de Lyon, Univ Claude Bernard, CNRS UMR 5239, INSERM U1210, Laboratory of Biology and Modelling of the Cell, 46 allée d'Italie Site Jacques Monod, F-69007, Lyon, France*

^c*Univ Lyon, Université Lyon 1, CNRS UMR 5208, Institut Camille Jordan, 43 blvd du 11 novembre 1918, F-69622 Villeurbanne-Cedex, France*

^d*Inria, Villeurbanne, France*

Abstract

Production of red blood cells involves growth-factor mediated regulation of erythroid progenitor apoptosis and self-renewal. During severe anemia, characterized by a strong fall of the hematocrit followed by a recovery phase, these controls allow a fast recovery of the hematocrit and survival of the organism. Using a mathematical model of stress erythropoiesis and an ad hoc numerical method, we investigate the respective roles of anemia-inducing phenylhydrazine injections and physiological regulation on the organism's recovery. By explicitly modeling the experimental protocol, we show that it mostly characterizes the fall of the hematocrit following the anemia and its severeness, while physiological process regulation mainly controls the recovery. We confront our model and our conclusions to similar experiments inducing anemia and show the model's ability to reproduce several protocols of phenylhydrazine-induced anemia. In particular, we establish a link between phenylhydrazine effect and the severeness of the anemia.

Keywords: erythropoiesis model, experimental protocol modeling, nonlinear age-structured system

*Corresponding author: crauste@math.univ-lyon1.fr

1. Introduction

Erythropoiesis, the process of production of red blood cells, is performed through complex regulatory processes, as part of the more general process of blood cell production. Red blood cells are produced in the bone marrow, where hematopoietic stem cells, that have abilities of self-renewal and differentiation in all blood cell types, generate immature erythroid cells called progenitors. Throughout successive differentiating divisions, erythroid progenitors acquire maturity to ultimately become mature red blood cells, called erythrocytes, that enter the bloodstream in order to carry oxygen to, and CO_2 from organs and tissues.

The continuous production of erythroid cells is permanently controlled in order to adapt very quickly to changes in, or needs of the organism. One of the main feedback controls, discovered in the early 1990's by Koury and Bondurant (1990), deals with erythroid progenitor death by apoptosis, a programmed cell death. Koury and Bondurant (1990) showed that, during an anemia (lack of red blood cells), a growth factor named erythropoietin (Epo) was released by the kidneys and inhibited progenitor apoptosis, allowing a fast production of numerous erythrocytes to recover from the anemia. This control of red blood cells upon their production is crucial for erythropoiesis regulation.

Apart from dying by apoptosis, erythroid progenitors experience differentiation in more mature cells or self-renew. Self-renewal (Watt and Hogan, 2000) is the ability of a cell to divide and give two daughter cells that have the same maturity than the mother cell, while keeping at all time the ability to engage in a differentiation process (i.e. to give two daughter cells, one of which at least being more mature than the mother cell). Self-renewal of erythroid progenitors has been shown during stress erythropoiesis (an anemia for instance) by Bauer et al. (1999), Gandrillon et al. (1999), and Pain et al. (1991). It is controlled by glucocorticoids, growth factors whose production negatively depends on the number of erythrocytes.

Several mathematical models of erythropoiesis have been proposed over the last 30 years, in order to address the regulatory mechanisms and their role in stress or pathological conditions. Bélair et al. (1995) proposed a model of erythropoiesis considering the influence of growth factors on stem cell differentiation in erythroid progenitors. This model was then improved by Mahaffy et al. (1998), and later analyzed in detail by Ackleh et al. (2002, 2006, 2008) and Banks et al. (2004). Another erythropoiesis model, inspired

38 by the same article, in which Epo is the only growth factor supposed to act
39 during erythropoiesis, was introduced in Adimy et al. (2006).

40 An important contribution to mathematical modeling of erythropoiesis
41 is also due to Loeffler and his collaborators (Loeffler and Wichmann, 1980;
42 Loeffler et al., 1989; Roeder, 2006; Roeder and Loeffler, 2002; Wichmann
43 and Loeffler, 1985; Wichmann et al., 1989). Their models consider feedback
44 controls from progenitors on the stem cell level and from mature cells on
45 progenitors, and are fitted to various experiments that induce severe anemias.
46 Most of these works were nevertheless performed before the role of Epo was
47 definitely identified and long before erythroid progenitor self-renewal was
48 hypothesized.

49 We proposed a new model of erythropoiesis (Crauste et al., 2008), based
50 on previous works by Mackey (1978) and co-authors, and Loeffler's group
51 (Loeffler et al., 1989; Roeder and Loeffler, 2002; Roeder, 2006), to describe
52 stress erythropoiesis in mice. This model is based on the description of ery-
53 throid progenitor and erythrocyte dynamics using delay equations. Progen-
54 itor apoptosis and self-renewal are regulated by the number of erythrocytes,
55 hence implicitly describing growth factor-mediated regulation. The model's
56 outputs were compared to data on phenylhydrazine-induced anemia in mice
57 and showed first that it was relevant and necessary to account for erythroid
58 progenitor self-renewal in order to explain experimental data. Second, they
59 showed that it was necessary to account for a modification of erythrocyte
60 lifespan after phenylhydrazine injections in order to reproduce the data, even
61 though this had not been assumed in the initial modeling. Phenylhydrazine
62 is a substance that kills circulating red blood cells but also damages sur-
63 viving red blood cell membranes and yields long term deficiency of the ery-
64 thropoiesis system (Walter et al., 1975). Notably, phenylhydrazine-induced
65 anemia is described in this model as a perturbation of the initial state of
66 the system and is hence not explicitly modeled. In particular, the biological
67 mechanisms involved in the reaction to phenylhydrazine injections are not
68 considered: it is a model of recovery from an anemia but not of anemia itself.

69 The way anemia is induced in mice influences the strength of the anemia
70 and the dynamics of the recovery. The two main ways of inducing anemia
71 are either to bleed mice in order to remove red blood cells, or to inject mice
72 with phenylhydrazine. Hematocrit values following bleeding-induced anemia
73 display smooth recovery dynamics, while following phenylhydrazine-induced
74 anemia they show a fast recovery phase that overcomes the initial hemat-
75 ocrit value and then slowly goes back to its initial state (see Figure 1), even

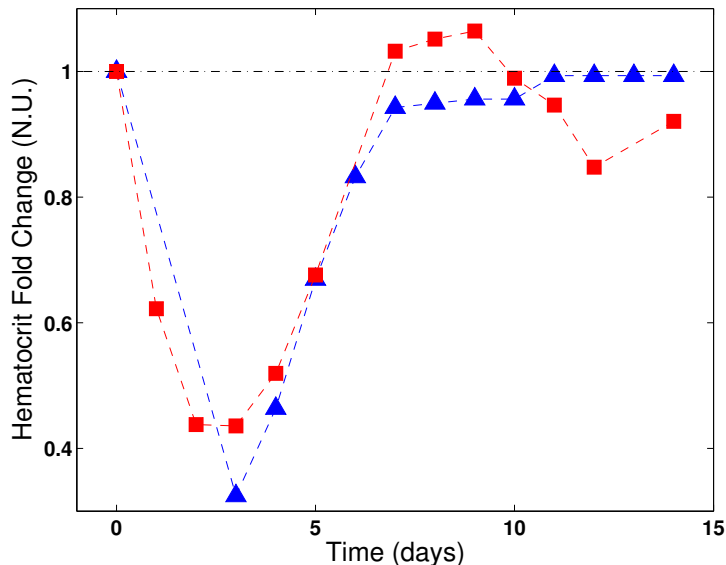


Figure 1: **Phenylhydrazine versus bleeding-induced anemia.** Hematocrits of mice submitted to severe anemia either by phenylhydrazine injections (red squares) or bleeding (blue triangles), mean fold change values are displayed (note that standard deviations are small and not visible using square and triangle symbols as well as normalized scales). The experimental protocol for phenylhydrazine-induced anemia is detailed in Section 2.3, for Group G0. Bleeding-induced anemia have been performed on 3 mice, each mouse was bled about 500 microliters with immediate injection of 500 microliters of intraperitoneal saline on three consecutive days (days 0, 1 and 2). Post-bleeding results were obtained with about 20 microliters of blood drawn on each day from day 3 (Eymard et al., 2015; Rhodes et al., 2016). These data are courtesy of Prof. Mark Koury, Vanderbilt University.

76 though the bleeding-induced anemia is more severe (minimum hematocrit
 77 value is about 30% of the initial hematocrit). This points towards differ-
 78 ent underlying physiological mechanisms associated to the anemia and its
 79 recovery.

80 We propose in this work a mathematical model of stress erythropoiesis in
 81 mice, based on the model of Crauste et al. (2008), which explicitly includes
 82 an age-dependent description of the experimental protocol used to induce
 83 a severe anemia, consisting in injecting mice with two consecutive doses of
 84 phenylhydrazine. The objective of the current work is to complete our pre-
 85 vious work (Crauste et al., 2008) by highlighting the respective roles of the

86 experimental protocol (here phenylhydrazine-induced anemia) and physiolog-
 87 ical processes in the induction of the anemia and its recovery. To do so, we
 88 consider an age-structured model of erythropoiesis in which an age-dependent
 89 red blood cell mortality rate is introduced to account for phenylhydrazine ef-
 90 fects. This model is presented in Section 2.1. We introduce the main features
 91 of the experimental data of phenylhydrazine-induced anemia in Section 2.3.
 92 We then use this framework to investigate in Section 3 the respective in-
 93 fluences of phenylhydrazine injections and of the physiological processes on
 94 the induction of the anemia (its strength and its duration) and the organism
 95 recovery.

96 2. Material, Methods, and Models

97 2.1. Mathematical Model

98 We introduce a mathematical model of stress erythropoiesis in mice, based
 99 on age-structured nonlinear partial differential equations describing erythroid
 100 progenitor and erythrocyte dynamics submitted to phenylhydrazine (PHZ)
 101 injections inducing anemia. This model is similar to the model introduced
 102 in Crauste et al. (2008), except for its description of PHZ injections.

Let consider a population of erythroid progenitors and a population of
 erythrocytes, characterized by cell age a and the time of the observation t (see
 Figure 2). Among progenitors, two populations are considered: self-renewing
 progenitors, whose population is denoted by $s(t, a)$, and differentiating pro-
 genitors, denoted by $p(t, a)$. All progenitors are supposed to be in the bone
 marrow and subject to death by apoptosis. The duration of the differen-
 tiating progenitor compartment is denoted by τ_p , and the duration of one
 self-renewing cycle by τ_c , with $\tau_c < \tau_p$. Erythroid progenitors are assumed
 to differentiate in erythrocytes when they reach the age $a = \tau_p$. The number
 of erythrocytes, circulating in blood, is denoted by $e(t, a)$, and $E(t)$ denotes
 the total number of erythrocytes at time t , defined by

$$E(t) = \int_0^{+\infty} e(t, a) da.$$

103 Denote by α the erythroid progenitor apoptosis rate, and by σ the ery-
 104 throid progenitor self-renewal rate. The rate α is assumed to be an increasing
 105 function of E , since the more erythrocytes the less erythropoietin (Koury and
 106 Bondurant, 1990), and erythropoietin inhibits erythroid progenitor apopto-
 107 sis (Koury and Bondurant, 1990). The rate σ is assumed to be a decreasing

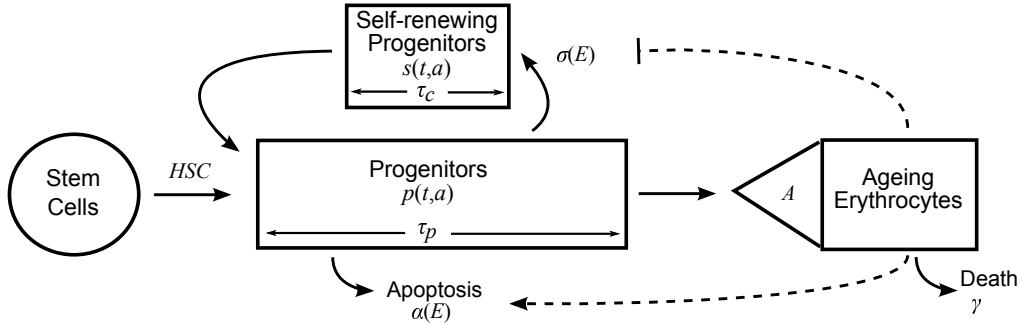


Figure 2: **Schematic representation of the erythropoiesis model.** Dashed lines represent feedback controls. See text for notations.

108 function of E : the more erythrocytes, the more glucocorticoids and the more
 109 glucocorticoids the less erythroid progenitor self-renewal (Bauer et al., 1999).

110 Denote by γ the mortality rate of erythrocytes. This rate depends on
 111 erythrocyte age a and time t when PHZ induces anemia, and is constant
 112 otherwise. In Crauste et al. (2008), we noticed that in order to correctly
 113 reproduce experimental data, a modification of the mortality rate of ery-
 114 throcytes had to be accounted for, as a consequence of using PHZ to induce
 115 anemia: one effect of this substance is to dramatically alter the lifespan of
 116 erythrocytes (Berlin and Lotz, 1951; Nagai et al., 1968, 1971; Shimada, 1975;
 117 Stohlman, 1961). Such a change in lifespan could be due to specific mem-
 118 brane properties of the erythrocytes produced during stress erythropoiesis
 119 (Walter et al., 1975). To account for this effect, it is necessary to explicitly
 120 describe PHZ injections: we hence define a nonnegative function phz that
 121 describes increases in the mortality rate γ following PHZ injections.

122 The function phz first depends on the age of erythrocytes a and the
 123 time of the observation t : erythrocytes already circulating in blood when
 124 PHZ is injected are affected by PHZ (they either die or are damaged), while
 125 erythrocytes produced after the injection are not affected by the PHZ and
 126 consequently their mortality rate is not modified. In addition, the function
 127 phz is characterized by the time of the injection, denoted by t_i , and by the
 128 duration of the PHZ effect in the blood (associated with the PHZ clearance

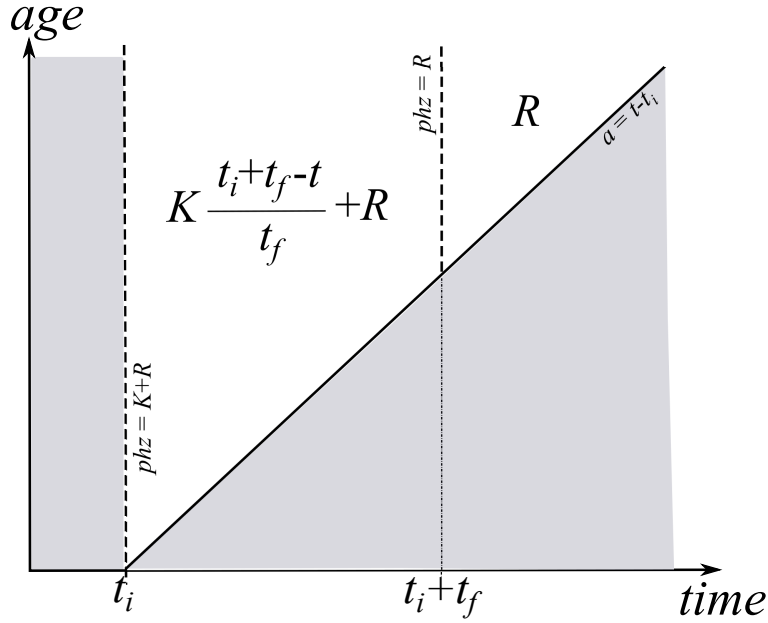


Figure 3: **Function** $(a, t) \mapsto phz(a, t, t_i, t_f)$, for fixed t_i and t_f . The grey areas correspond to $phz = 0$. Along the vertical dashed lines, phz is equal to its maximum ($phz = K + R$, on the left line) or to its minimum ($phz = R$, on the right line).

129 rate), denoted by t_f . We define, for $a, t \geq 0$,

$$phz(a, t, t_i, t_f) = \begin{cases} 0, & t \leq t_i \text{ or } a \leq t - t_i, \\ K \frac{t_i + t_f - t}{t_f} + R, & t_i \leq t \leq t_i + t_f \text{ and } a \geq t - t_i, \\ R, & t_i + t_f \leq t \text{ and } a \geq t - t_i. \end{cases} \quad (1)$$

130 The function phz is also characterized by a nonnegative residual effect R ,
 131 and a positive constant K which determines the maximum effect of the PHZ
 132 injection on the mortality rate of erythrocytes. A positive residual effect R
 133 means that erythrocytes that did not die following the PHZ injection have a
 134 larger mortality rate than cells that never encountered PHZ due to membrane
 135 damages, even though the organism is cleared with PHZ (Walter et al., 1975).
 136 A schematic representation of the effect of the phz function is illustrated in
 137 Figure 3.

138 In order to compare the model simulations with experimental data (see
 139 Sections 2.3 and 2.4), we reproduce the experimental protocol consisting

140 in two injections, following closely one another, with the initial injection
 141 occurring at time $t_i = t_1 = 0$ and the second injection at time $t_i = t_2 > 0$.
 142 Since experimentally both injections are similar (same dose, same route of
 143 injection), we assume that they both have the same effects and we use the
 144 same parameter values for the function phz , except for the value of t_2 .

145 We use the notation $\gamma(t, a)$ to stress the time and age-dependency of the
 146 PHZ-based experimental protocol, with

$$\gamma(t, a) = (1 + phz(a, t, 0, t_f) + phz(a, t, t_2, t_f)) \bar{\gamma}, \quad (2)$$

147 where $\bar{\gamma}$ stands for the average erythrocyte mortality rate.

148 Then, the quantities p , s and e satisfy the following system, for $t > 0$,

$$\begin{cases} \partial_t p(t, a) + \partial_a p(t, a) = -[\alpha(E(t)) + \sigma(E(t))] p(t, a), & a \in (0, \tau_p), \\ \partial_t s(t, a) + \partial_a s(t, a) = -\alpha(E(t)) s(t, a), & a \in (0, \tau_c), \\ \partial_t e(t, a) + \partial_a e(t, a) = -\gamma(t, a) e(t, a), & a > 0. \end{cases} \quad (3)$$

149 Boundary conditions associated with (3) describe cell flux between compart-
 150 ments,

$$\begin{cases} p(t, 0) = HSC + 2s(t, \tau_c), \\ s(t, 0) = \int_0^{\tau_p} \sigma(E(t)) p(t, a) da, \\ e(t, 0) = Ap(t, \tau_p). \end{cases} \quad (4)$$

151 New erythroid progenitors come from the division of self-renewing progeni-
 152 tors and the differentiation of hematopoietic stem cells: HSC denotes the
 153 constant flux of hematopoietic stem cells differentiating in erythroid progeni-
 154 tors. Self-renewing progenitors are produced at a rate σ . Erythrocytes are
 155 produced from mature (age $a = \tau_p$) progenitors, and A denotes a constant
 156 amplification coefficient accounting for divisions of mature progenitors. For
 157 instance, $A = 2^d$ where d is the number of differentiation compartments
 158 during the reticulocyte stage (Crauste et al., 2008).

159 Existence and uniqueness of solutions of system (1)–(4) follow from the
 160 classical theory of age-structured equations (Webb, 1985), under conditions of
 161 smoothness of the nonlinear feedback functions α and σ . In addition one can
 162 show that system (3)–(4) has a unique steady state (a constant solution with
 163 respect to time t) under appropriate conditions (see Angulo et al. (2017), for
 164 a more general model). However, it must be noted that the complexity of the
 165 mathematical model limits the theoretical analysis that can be performed.

166 *2.2. Numerical Simulations*

167 The effort made on increasing the realism in the model is achieved at the
 168 expense of loss in mathematical tractability. Let's point out that, without
 169 additional restrictive assumptions, system (1)–(4) cannot be solved analyti-
 170 cally. Therefore the use of efficient methods providing a numerical approach
 171 is the most suitable mathematical tool for studying the model and, indeed,
 172 it is often the only one available. Besides, numerical methods have been
 173 successfully applied to structured models to replicate available field and/or
 174 laboratory data for a variety of different systems (e.g. Angulo and López-
 175 Marcos (2012); Angulo et al. (2011a,b, 2013a,b)). We completely describe
 176 in Angulo et al. (2017) the explicit second order numerical scheme built “ad
 177 hoc”, which has been adapted to obtain the solutions of system (1)–(4).

178 When performing numerical simulations, we use the functions

$$\alpha(E) = C_\alpha \frac{E^{n_\alpha}}{\theta_\alpha^{n_\alpha} + E^{n_\alpha}}, \quad \text{and} \quad \sigma(E) = C_\sigma \frac{\theta_\sigma^{n_\sigma}}{\theta_\sigma^{n_\sigma} + E^{n_\sigma}}, \quad (5)$$

179 where $C_\alpha, C_\sigma > 0$ are the maximal apoptosis and self-renewal rates, respec-
 180 tively, $\theta_\alpha, \theta_\sigma > 0$ threshold values, and $n_\alpha, n_\sigma > 1$ sensitivity parameters.

181 In order to compare the model's outputs with experimental data (see
 182 Section 2.3), the numerical solution of system (1)-(4) is used to compute the
 183 simulated hematocrit HCT , using the formula (Crauste et al., 2008)

$$HCT(t) = \frac{E(t)}{E(t) + E^*(1 - HCT^*)/HCT^*}, \quad (6)$$

184 where $E(t)$ is the total number of erythrocytes and HCT^* is the steady state
 185 value of the hematocrit, obtained through experimental data.

186 *2.3. Experimental Data*

187 In order to get some insights into stress erythropoiesis, experiments con-
 188 sisting in inducing an anemia in mice and monitoring the recovery have been
 189 performed. Let us remind the reader that “hematocrit” is a test that mea-
 190 sures the volume of red blood cells in a blood sample. It gives a percentage
 191 of erythrocyte volume found in the whole blood volume. Since platelet and
 192 white cell volumes are negligible within a blood sample, we assumed without
 193 loss of generality that a blood sample is mainly composed with erythrocytes
 194 and plasma.

195 Figure 4 shows the time evolution of the hematocrit of 5 batches of adult
 196 mice (groups G0 to G4), over 17 days, being rendered anemic by two consec-
 197 utive intraperitoneal injections of PHZ with different doses. Even though the
 198 5 batches display quantitative differences, they all reproduce the main basic
 199 features: Initially at its steady value, between 45 and 55 %, the hematocrit
 200 shows a strong fall following the anemia (the hematocrit reaches very low
 201 values, about $23\% \pm 3\%$, 2 to 3 days after the first injection for G0), then
 202 rapidly increases to reach a high value (about $55\% \pm 4\%$, 9 days after the first
 203 injection, for G0), and then returns to the equilibrium. Note that data for
 204 group G0 come from Crauste et al. (2008).

205 Experiments performed on groups G0 to G4 vary in the dose of PHZ used
 206 to induce the anemia: G0 mice were injected with a 60mg/kg body weight
 207 dose, while G1, G2, and G3 mice were injected with a 30 mg/kg body weight
 208 dose and G4 mice with a 15 mg/kg body weight dose. They also differ with
 209 respect to the time of the second injection: G0, G1 and G4 mice were injected
 210 on days 0 and 1, G2 mice on days 0 and 0.7 (16h), and G3 mice on days 0
 211 and 2. See Figure 4.C for a summary of these protocols.

212 In order to characterize the strength of the PHZ-induced anemia, we
 213 introduce the following quantities:

- 214 - HCT_{min} , the minimum value of the hematocrit ($HCT_{min} \approx 23 \pm 3\%$
 215 for group G0),
- 216 - t_{min} , the time after the initial injection at which the minimum of the
 217 hematocrit is reached ($t_{min} \approx 3$ days for group G0),
- 218 - t_{rec} , the recovery time, which is the first time the hematocrit reaches a
 219 given value (we chose the value 40%, which is just below the equilibrium
 220 value), after the hematocrit reached a minimum ($t_{rec} \approx 6$ days for group
 221 G0).

222 The first quantity directly measures the strength of the anemia, because the
 223 smaller the hematocrit the higher the probability that the organism cannot
 224 recover (and then eventually dies). The second quantity relates to the initial
 225 resistance of the organism to the anemia, and measures the speed at which
 226 the hematocrit decreases. The third quantity is related to the ability of the
 227 organism to recover from the anemia, and it measures the velocity at which
 228 the hematocrit recovers. A “strong” anemia will then be characterized first
 229 by a low minimum of the hematocrit, and second by a short time to reach

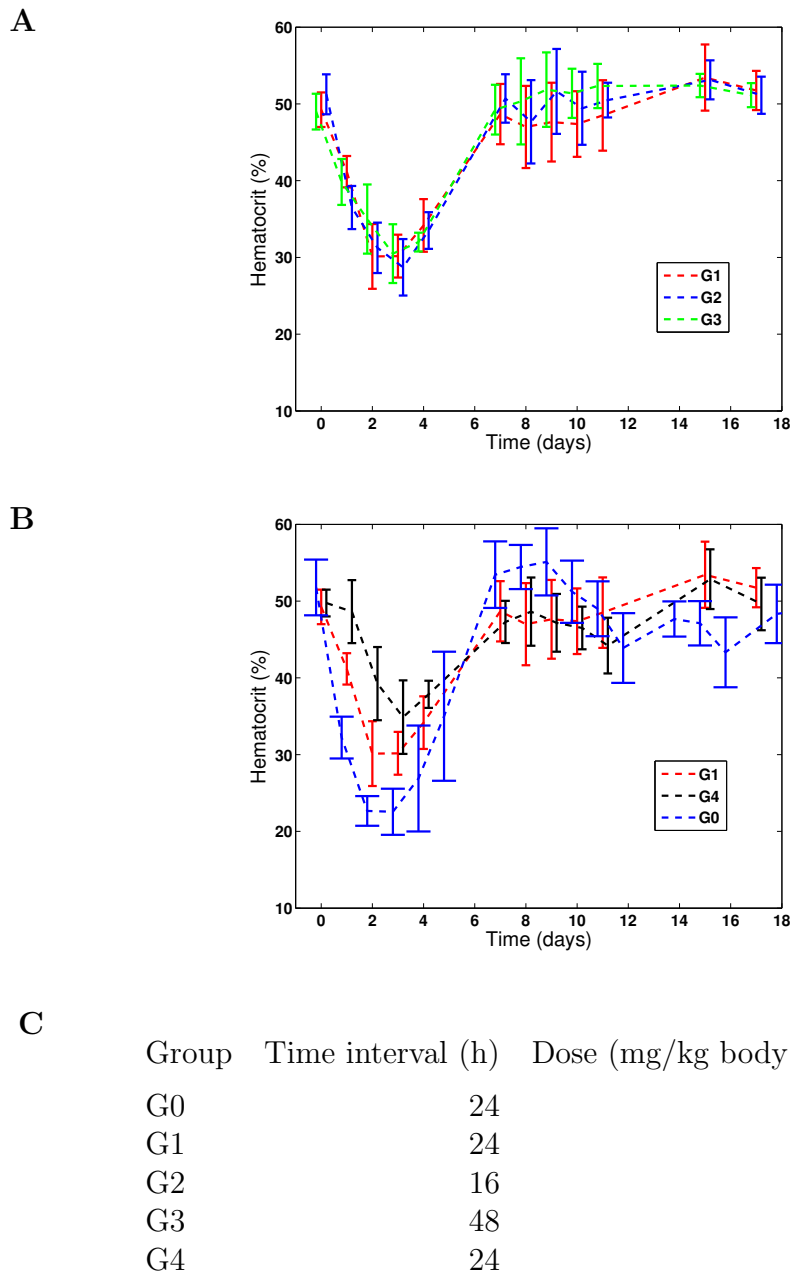


Figure 4: **Experimentally measured hematocrits.** Hematocrits of groups **(A)** G1 (red), G2 (blue), G3 (green), and **(B)** G1 (red), G4 (black), G0 (blue). Average and standard deviations over 9 (group G0) or 8 (groups G1 to G4) adult mice are displayed on the 17 days period. **(C)** Characteristics of PHZ-induced anemia experiments: for each of the 5 groups, the time interval between two consecutive injections of PHZ and the dose that has been injected are presented.

230 this minimum. Potentially, one can also add to this definition a long time
 231 of recovery and a slow speed of recovery, while keeping in mind that the
 232 organism has to react quickly otherwise its survival can be questioned. A
 233 “weak” anemia on the contrary will be characterized by a high minimum of
 234 the hematocrit.

235 2.4. Parameter Estimation

236 We proceed in two steps. We first use data from group G0 to estimate
 237 parameter values and evaluate the contribution of each parameter to the
 238 quality of the results. Second, we investigate the robustness of the model by
 239 confronting it, and estimated parameter values, to data from groups G1 to
 240 G4 (see Section 2.3).

In the first step, we first estimate parameter values so that the model
 correctly reproduces experimental data from group G0. We simulate the
 model for fixed parameter values and compute the weighted residual sum of
 squares using G0 data. The weighted residual sum of squares is given by

$$RSS := \sum_{i=1}^N \frac{(SimulatedHCT_i - ExperimentalHCT_i)^2}{\sigma_i^2},$$

241 where N is the size of the experimental sample, $SimulatedHCT_i$ the value of
 242 the simulated hematocrit at the i -th experimental time, $ExperimentalHCT_i$
 243 the corresponding average hematocrit value, and σ_i the experimental stan-
 244 dard deviation. The same formula is used for groups G0 to G4, using each
 245 time corresponding data. Identifiability of estimated parameter values (Raue
 246 et al., 2009) is deduced from the boundedness of 95% confidence intervals,
 247 hence estimated parameter values indeed correspond to a global minimum of
 248 the residual sum of squares.

249 This leads us to identify parameter values that best reproduce G0 data,
 250 and situations that favor quantitatively relevant dynamics. We then focus
 251 on the contribution of some parameters to the severity of the anemia and
 252 the recovery’s features. The complexity of the model limits the numerical
 253 analysis, so it would not be reasonable to try performing a sensitivity analysis
 254 on every parameter of the model. This is why we focus on the influence of
 255 specific parameters, which characterize the main feedback functions of the
 256 system, on the model’s features. To that aim, we vary them individually in
 257 a given range while fixing the others. For each parameter, the range used as
 258 well as the paragraph presenting the results are indicated in Table 1.

Table 1: **Parameter sensitivity ranges.** For each parameter of interest (column ‘Parameter’) the prospective interval in which its influence on the dynamics of the model is investigated appears in the column ‘Range’, and the subsection label in which these results are presented in the column ‘Paragraph’. The upper part of the table deals with the 9 parameters whose values are also estimated to fit the data, while the bottom part of the table deals with the 4 parameters whose values are fixed throughout simulations.

Parameter	Range	Paragraph	Parameter	Range	Paragraph
C_α	[0; 70]	<i>not shown</i>	C_σ	[0; 4]	3.4
θ_α	$[10^4; 10^8]$	3.3	θ_σ	$[10^4; 10^8]$	<i>not shown</i>
n_α	[1; 58]	<i>not shown</i>	n_σ	[1; 35]	<i>not shown</i>
R	[0; 8]	3.2	t_f	[0; 5]	3.2
t_2	[0; 2]	3.2			
τ_p	[1; 8]	3.3	τ_c	$[0; \tau_p]$	<i>not shown</i>
HSC	$[10^2; 10^6]$	3.5	A	[100; 500]	<i>not shown</i>

259 In the second step, we use the estimated parameter values to confront our
 260 model to data from groups G1 to G4, in order to evaluate its robustness in
 261 describing different dynamics obtained with very similar experimental pro-
 262 tocols. In order to characterize each group dynamics, we also compute the
 263 weighted residual sum of squares.

264 While most parameter values will be estimated to reproduce experimen-
 265 tal data, some values will be fixed throughout the parameter estimation
 266 procedure, both in steps 1 and 2 (these parameters are however varied for
 267 investigating the potential influence of their variation on the system’s behav-
 268 ior).

269 The average lifespan of an erythrocyte is known to be 40 days in mice
 270 (Crauste et al., 2008), so the average mortality rate would be $\bar{\gamma} = 1/40 \text{ d}^{-1}$.
 271 Values of the amplification coefficient of progenitors into erythrocytes A , and
 272 of HSC flux into the erythroid lineage HSC , are taken from Crauste et al.
 273 (2008), $A = 2^8$ and $HSC = 10^4 \text{ cells.vol}^{-1}$ respectively. Also, the progenitor
 274 compartment duration τ_p and the cell cycle duration τ_c are fixed to $\tau_p = 4$
 275 days and $\tau_c = 1$ day (Crauste et al., 2008).

276 Additionally parameter K in (1) is fixed to $K = 20 \text{ d}^{-1}$, after multiple
 277 tests showed no real influence of variations of K . Finally, the simulation step

278 h is fixed throughout all simulations to $h = 1/128$ day (see Angulo et al.
279 (2017)).

280 **3. Results**

281 We use the model presented in Section 2 to simulate a PHZ-induced
282 anemia in mice and the response of the organism, and we mainly focus on
283 two points. First, we investigate the influence of the experimental protocol
284 upon the features (strength, duration) of the anemia. Second, we evaluate
285 the roles of physiological processes regulating erythrocyte production. To do
286 so, we compare results of the simulations of system (1)-(4) with experimental
287 data presented in Section 2.3, group G0. We then show that our model is able
288 to describe other experimental data (groups G1 to G4) and draw conclusions
289 about PHZ-induced anemia.

290 *3.1. Data*

291 Hematocrit evolves similarly for groups G1, G2 and G3 (see Figure 4.A).
292 Quantitative differences are however important between the hematocrits of
293 groups G0, G1, G4, for which the injected doses of PHZ are different (see
294 Figure 4.B). Both the fall of the hematocrit phase and the recovery phase
295 display different features, which appear to be dose-dependent: distinct values
296 of the minimum value of the hematocrit and different slopes of the recovery
297 phase. Additionally, high values observed for group G0 around day 9 are
298 not observed for the other groups. As mentioned in Crauste et al. (2008),
299 these high values appear to be caused by a strong reaction of the organism
300 that needs to quickly produce new red blood cells in order to ensure survival
301 associated with a lag (or inertia) in the regulation of progenitor apoptosis
302 that does not compensate fast enough this production of new red blood cells,
303 resulting in an overshoot of the hematocrit.

304 *3.2. Influence of PHZ injections*

305 In order to investigate the influence of the injection protocol on the dy-
306 namics of stress erythropoiesis and blood recovery, we focus on 3 parameters
307 (see Section 2.1), namely

- 308 - R , the residual influence of PHZ injections,
- 309 - t_f , the duration after which only the residual effect of PHZ is felt by
310 the organism,

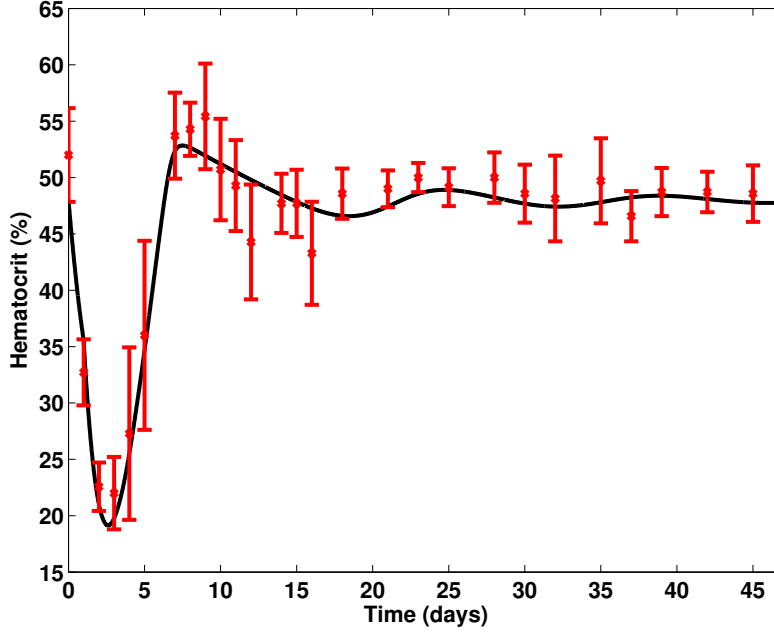


Figure 5: **Experimental and simulated hematocrits for group G0.** Experimental data are given by the red crosses with bars (mean value \pm standard deviation). The simulated hematocrit is given by the black curve. All estimated parameter values are from Table 2.

311 - t_2 , the time of the second injection (the initial injection occurs at $t = 0$).

312 System (1)-(4) is numerically solved and the corresponding simulated
 313 hematocrit HCT is computed using (6). The simulation that best reproduces
 314 experimental data for group G0 is shown in Figure 5. It has been obtained
 315 with $R = 5 \text{ d}^{-1}$, $t_f = 3$ days, $t_2 = 1$ day, while other parameter values are
 316 given in Table 2. This set of parameter values for (R, t_f, t_2) is characteristic of
 317 a “good” situation: the model correctly reproduces experimental data when
 318 $t_f \geq 2$ days and

319 - either the residual effect R is large ($R \geq 3 \text{ d}^{-1}$),

320 - or R is small ($1 \text{ d}^{-1} < R \leq 3 \text{ d}^{-1}$), provided that the smaller R the
 321 larger t_f , and t_2 is not too large ($t_2 \leq 1.5$ days).

Table 2: **Parameter values corresponding to Figure 5.** All parameter values listed in the table have been estimated: the best value is indicated in the column ‘Value’ while its 95% confidence interval is indicated in the column ‘Confidence Interval’. Key: vol = volume unit; N.U. = no unit.

Parameter	Value	Confidence Interval	Unit
<i>Apoptosis Rate</i>			
C_α	20	[19.6; 20.4]	d ⁻¹
θ_α	10 ^{6.5}	[10 ^{6.4} ; 10 ^{6.6}]	cells.vol ⁻¹
n_α	10.6	[10.4; 10.8]	N.U.
<i>Self-Renewal Rate</i>			
C_σ	0.7	[0.63; 0.77]	d ⁻¹
θ_σ	10 ^{6.8}	[10 ^{6.6} ; 10 ^{7.0}]	cells.vol ⁻¹
n_σ	6.2	[5.8; 6.6]	N.U.
<i>PHZ Injections</i>			
R	5	[4.9; 5.1]	d ⁻¹
t_f	3	[2.95; 3.04]	d
t_2	1	[0.97; 1.03]	d

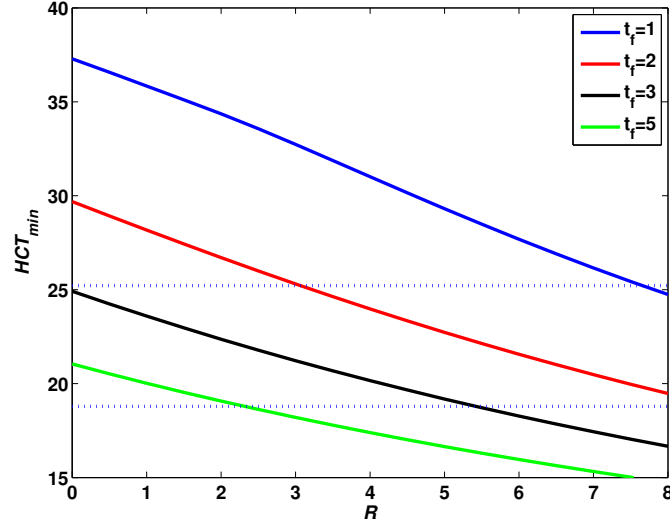
322 These situations are a priori biologically realistic. The first one corresponds
323 to a strong effect of PHZ on erythrocytes that survived the first injection,
324 while the second one corresponds to a second injection following quickly the
325 first one in order to sustain the action of PHZ. One may note that, in the
326 experiments, $t_2 = 1$ day which is in agreement with our estimation, while no
327 information on neither R nor t_f is available.

328 When $R = 0$ or R is close to zero, the model is unable to correctly describe
329 the fall of the hematocrit that follows the two injections, and varying K in (1)
330 does not improve the results, since the organism always reacts much faster
331 in this case than what is experimentally observed (data not shown). This
332 indicates that the residual effect plays an important role in inducing severe
333 anemia, following PHZ injections, as suggested in Crauste et al. (2008).

334 We further investigate the roles of R , t_f and t_2 by focusing on specific
335 features of the anemia: HCT_{min} , t_{min} and t_{rec} .

336 Parameters R and t_f have a major influence on the strength of the ane-

A



B

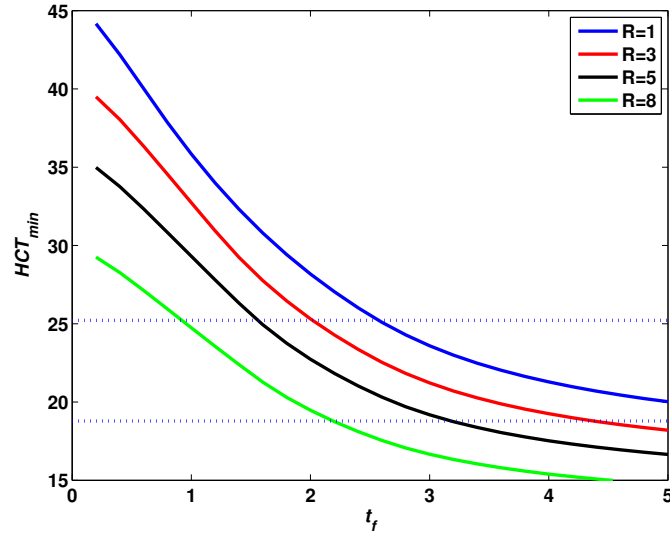


Figure 6: **Influence of the values of R and t_f on the values of HCT_{min} .** Values of HCT_{min} are computed for $t_2 = 1$ day and **(A)** $R \in [0, 8] \text{ d}^{-1}$, with $t_f = 1$ day (blue curve), $t_f = 2$ days (red curve), $t_f = 3$ days (black curve), $t_f = 5$ days (green curve), and **(B)** $t_f \in [0.2, 5]$ days, with $R = 1 \text{ d}^{-1}$ (blue curve), $R = 3 \text{ d}^{-1}$ (red curve), $R = 5 \text{ d}^{-1}$ (black curve), $R = 8 \text{ d}^{-1}$ (green curve). Black dash-dotted lines indicate the range of experimental values of HCT_{min} (from Figure 5, group G0). Other parameter values are given by Table 2.

337 mia. The minimal hematocrit value, HCT_{min} , is mainly controlled by R
 338 and t_f (Figure 6): the larger R and t_f , the lower HCT_{min} and the more
 339 severe the anemia. In addition, combined increases of R and t_f strengthen
 340 the anemia by more strongly decreasing HCT_{min} than each parameter sep-
 341 arately. This complements the above conclusion regarding the obtention of
 342 good reproduction of data: for large values of both R and t_f the simulated
 343 solution correctly reproduces experimental data, and in particular it correctly
 344 captures the value of the hematocrit at its minimum.

345 Second, the time at which the second injection occurs, t_2 , is the main
 346 parameter controlling the time at which the hematocrit reaches its minimum
 347 value, t_{min} (Figure 7): t_{min} increases as t_2 increases. This influence of t_2
 348 on t_{min} indicates that the organism does not react fast enough to the first
 349 injection to limit the action of the second injection. The residual effect R
 350 shows very limited influence on the value of t_{min} . The parameter t_f shows no
 351 influence on t_{min} , except for situations that have been identified as unable to
 352 generate a correct response to the anemia (small values of t_f , R and t_2). In
 353 conclusion, t_2 strongly influences t_{min} , whereas R and t_f have either limited
 354 or no influence on t_{min} .

355 None of these three parameters is however significantly influencing the
 356 recovery (Supp. Fig. 1 to 3), which remains fairly constant for all values
 357 of the three parameters (around 4.5-5.5 days). We then hypothesize that
 358 the recovery is mainly determined by the response of the organism to the
 359 anemia, and the investigation of the roles of physiological processes in the
 360 next sections will indeed confirm this hypothesis.

361 *3.3. Apoptosis and Differentiation Processes drive the Recovery*

362 The apoptosis rate α is characterized by three parameters: C_α , θ_α and
 363 n_α , see (5). The parameter C_α controls the maximum value of the apoptosis
 364 rate. It barely affects the strength of the anemia or the recovery time, except
 365 for extremely small and biologically unrealistic values (Supp. Fig. 4.A). The
 366 same conclusions hold for n_α , the sensitivity of the apoptosis rate (Supp. Fig.
 367 4.B). On the contrary, θ_α , that defines the strength of the Epo-mediated red
 368 blood cell control on progenitor apoptosis, clearly shows a strong influence on
 369 both HCT_{min} and t_{rec} : from Figure 8.A, one observes that HCT_{min} decreases
 370 and t_{rec} increases as θ_α increases. This indicates how controlling the apoptosis
 371 rate of erythroid cells strongly contributes to the dampening of an anemia and
 372 a fast recovery, stressing the key role of Epo-dependent regulatory processes
 373 in erythropoiesis.

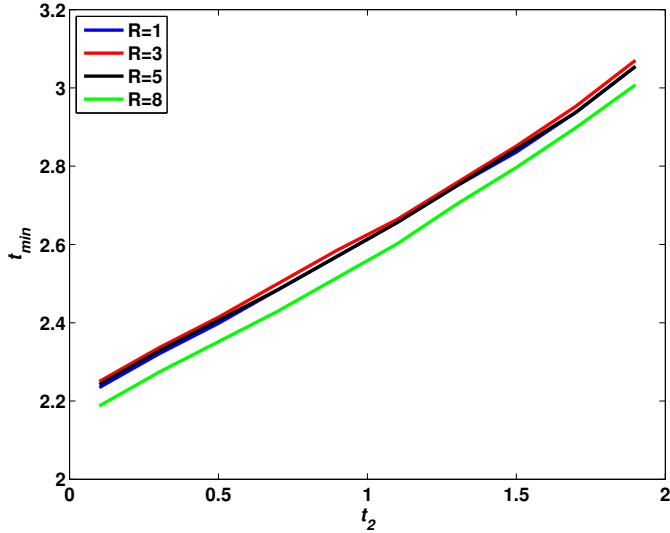


Figure 7: **Influence of the value of t_2 on the values of t_{min} .** Values of t_{min} are computed for $t_2 \in [0.1, 1.9]$ days, with $R = 1 \text{ d}^{-1}$ (blue curve), $R = 3 \text{ d}^{-1}$ (red curve), $R = 5 \text{ d}^{-1}$ (black curve), $R = 8 \text{ d}^{-1}$ (green curve), and $t_f = 3$ days. Other parameter values are given by Table 2.

374 Differentiation of erythroid progenitors is characterized by the differentia-
 375 tion time τ_p . Figure 8.B shows that long differentiation times first contribute
 376 to strong anemias and second, slow down recovery. The differentiation time
 377 τ_p , although not dependent on a feedback control in this model (no biolog-
 378 ical evidence), appears to play a role almost as important as the apoptosis
 379 rate in controlling the recovery. Shortening the differentiation process might
 380 be an efficient way to rapidly recover from a strong anemia. However, to
 381 our knowledge, a reduction of the duration of the differentiation process has
 382 never been experimentally observed in stress erythropoiesis, contrary to a
 383 control of the apoptosis rate by the number of circulating red blood cells.

384 3.4. Comments on the Role of the Self-Renewal Rate

385 Let us focus on the contribution of the self-renewal rate σ to the or-
 386 ganism's recovery from an anemia. The rate σ is characterized by three
 387 parameters C_σ , θ_σ and n_σ ,

388 First, C_σ has no significant influence on HCT_{min} and t_{min} (Supp. Fig.
 389 5), and consequently does not contribute to the severeness of the anemia.

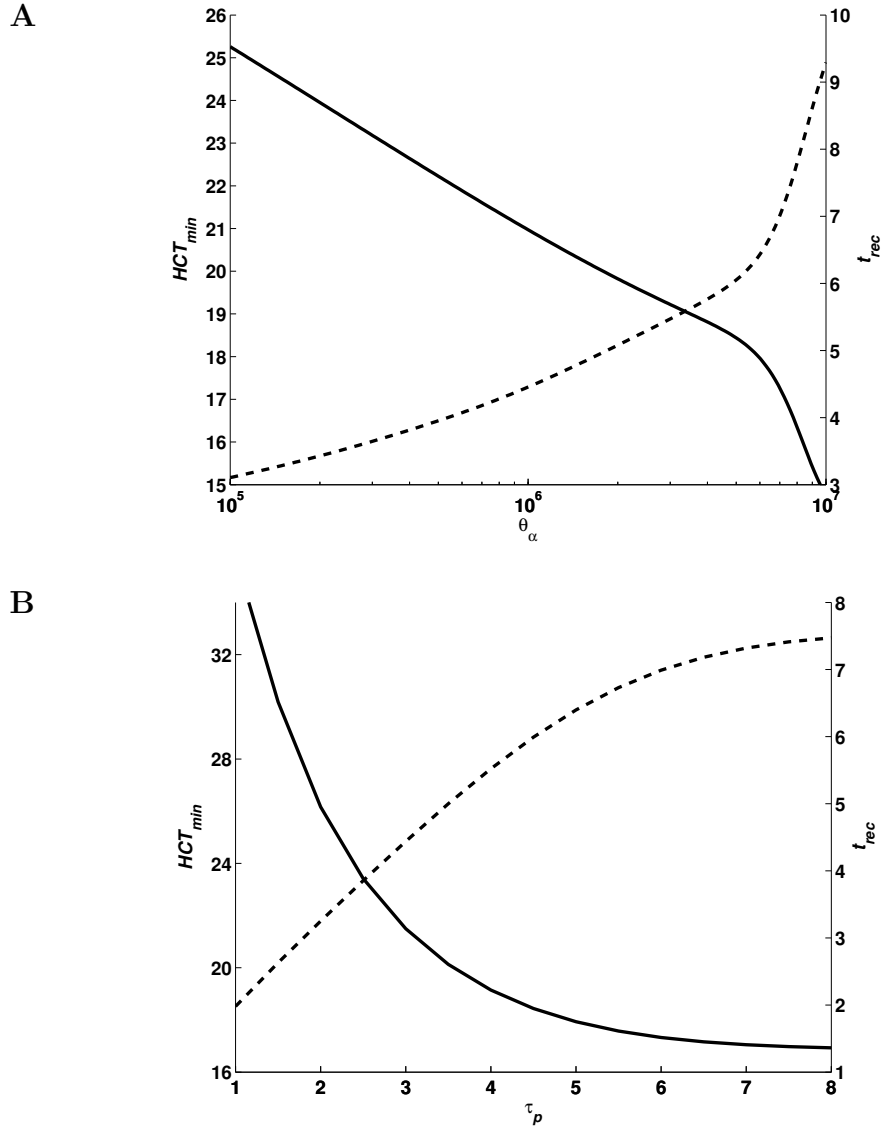


Figure 8: **Influence of θ_α and τ_p on HCT_{min} and t_{rec} .** (A) Influence of θ_α on HCT_{min} and t_{rec} . (B) Influence of τ_p on HCT_{min} and t_{rec} . In both cases, values of HCT_{min} are displayed on the left axis and correspond to the plain curve, while values of t_{rec} are displayed on the right axis and correspond to the dashed curve.

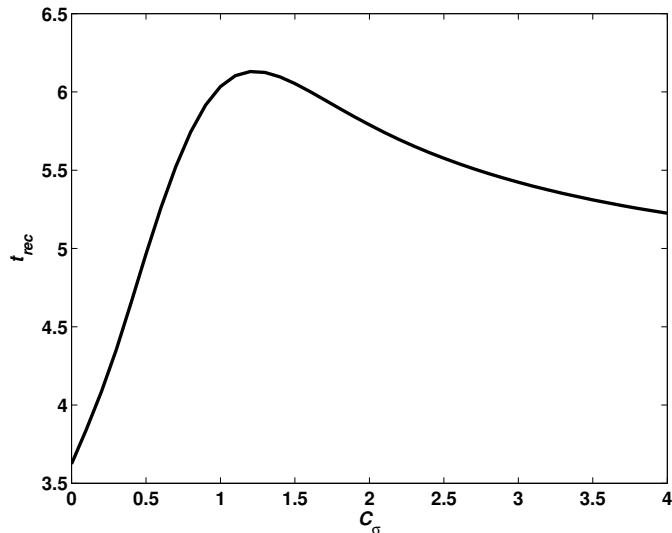


Figure 9: **Influence of C_σ on t_{rec} .**

390 Second, for small values of C_σ ($< 0.5 \text{ d}^{-1}$) one observes fast recoveries, char-
 391 acterized by $t_{rec} \leq 5$ days, while larger values of C_σ are associated with slow
 392 recoveries (see Figure 9). Other parameters associated with the self-renewal
 393 rate have a very limited influence (θ_σ) or no influence at all (n_σ) on both the
 394 anemia and the recovery (Supp. Fig. 6 and 7).

395 Even though self-renewal appears to be mandatory to recover from the
 396 anemia (in agreement with Crauste et al. (2008)), these results indicate that
 397 the regulation of the self-renewal rate (characterized by parameters θ_σ and
 398 n_σ) does not play a crucial role in the recovery and is potentially dispens-
 399 able. Consequently, we may hypothesize that the self-renewal rate is indeed
 400 constant among the erythroid progenitor population, equal to C_σ .

401 3.5. Comments on Stem Cell Regulation

402 The erythropoiesis process depends upon the production of immature
 403 erythroid progenitors by hematopoietic stem cells. This process is highly
 404 controlled (see for instance Pujol-Menjouet et al. (2005); Roeder and Loeffler
 405 (2002)), even though we did not model it in details since it is not part of
 406 the erythropoiesis process. We can however focus on the influence of the
 407 parameter associated with a continuous and constant production of erythroid
 408 progenitors, *HSC*.

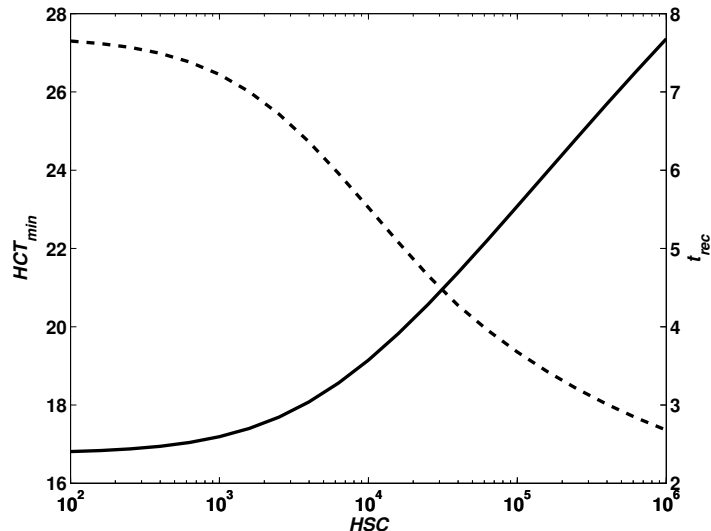


Figure 10: **Influence of HSC on HCT_{min} and t_{rec} .** HCT_{min} values are on the left axis and represented by the plain curve, while t_{rec} values are on the right axis and represented by the dashed curve. Note that HSC is represented in logarithmic scale on the x-axis.

409 Variations of this parameter show important modifications of HCT_{min}
 410 and t_{rec} (Figure 10), and of t_{min} (Supp. Fig. 8), indicating a significant
 411 influence of HSC both on the strength of the anemia and on the recovery.

412 Even though we cannot exclude that the entire recovery process could be
 413 controlled by the regulation of HSC dynamics, strong variations of the flux
 414 of HSC entering the erythroid lineage are usually associated with hematolog-
 415 ical disorders or diseases (Mackey, 1978; Pujo-Menjouet and Mackey, 2004).
 416 Hence, only small variations of the parameter HSC should be considered,
 417 and in this case the contribution of the regulation of the HSC compartment
 418 would be much less significant and essential to stress erythropoiesis.

419 Moreover, the regulation of HSC dynamics, leading to a modification of
 420 the flux of newly created erythroid progenitors, would not have instantaneous
 421 consequences on the erythropoiesis process: it would take several divisions,
 422 hence several days, to significantly modify the flux of stem cells differentiating
 423 in erythroid progenitors. One can observe on Figure 5 that the organism
 424 recovers 2 to 3 days after reaching its lowest level, a priori excluding the
 425 HSC regulation as the only mechanism allowing a fast recovery.

Table 3: **Estimated values of R and t_f for groups G1 to G4.** Values of R and t_f for group G0 are recalled for comparison purposes (in gray).

Group	R (d ⁻¹)	t_f (d)
G0	5	3
G1	0	2.2
G2	6	1
G3	0	3
G4	4.5	0.2

426 3.6. Reproducing various PHZ-induced anemia protocols

427 The above-mentioned analysis has been performed with parameter values
 428 that were estimated to reproduce experimental data from group G0. One
 429 may question the robustness of these values and their relevance in describ-
 430 ing stress erythropoiesis dynamics in other PHZ-induced anemia protocols.
 431 Groups G1 to G4 display similar features than group G0: fall of the hema-
 432 tocrit following PHZ injections, then a recovery period with a return to a
 433 steady hematocrit by day 17 post-injection ; yet they quantitatively behave
 434 differently depending on the dose (G1, G2, G3 *vs* G4) or the time between
 435 two injections (G1, G4 *vs* G2 *vs* G3). Since parameters R and t_f have been
 436 identified in Section 3.2 as responsible for the strength and duration of the
 437 anemia, we focus on their contribution in reproducing experimental data.

438 To investigate the model's behavior when used to reproduce data in
 439 groups G1 to G4, we first fix all parameter values associated with physi-
 440 ological processes to values obtained with the G0 group (Table 2), and we
 441 only vary parameters associated with PHZ injections: R and t_f . Value of the
 442 parameter t_2 is set according to the group ($t_2 = 1$ day for G1 and G4, $t_2 = 0.7$
 443 day for G2, and $t_2 = 2$ days for G3). Parameters R and t_f are determined to
 444 fit the data (see Table 3). Results are presented in Figure 11 by dashed lines.
 445 For each group, estimating only values of R and t_f does not provide correct
 446 reproduction of experimental data: although the anemia is rather properly
 447 described, the recovery is mostly overestimated whatever the group (too fast
 448 for all groups, and reaching values higher than experimental ones for groups
 449 G1, G2 and G4), and the simulated dynamics of the hematocrit are not in
 450 agreement with experimental observations.

451 In a second step, in addition to parameters R and t_f , we allow parameters

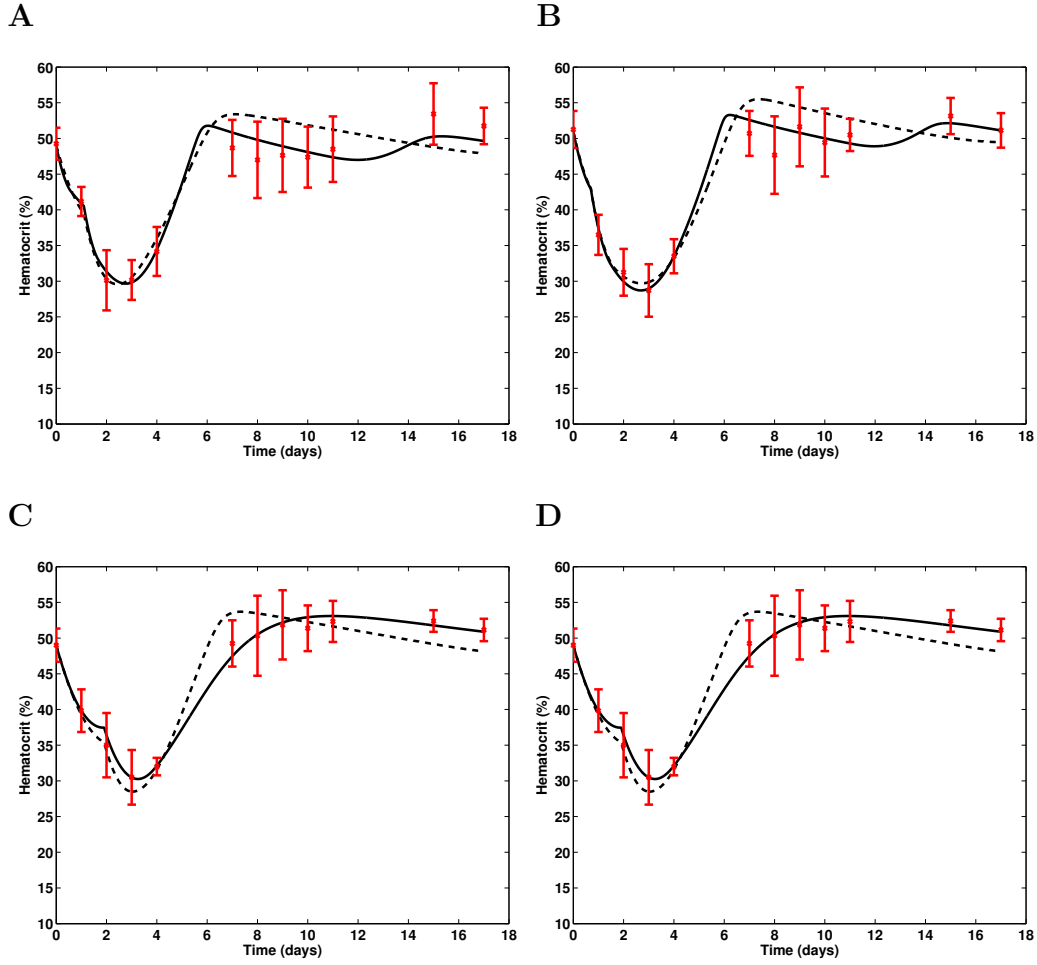


Figure 11: **Estimation of hematocrit dynamics for groups G1 (A), G2 (B), G3 (C) and G4 (D).** For each figure, the value of t_2 is fixed according to the experimental protocol. The solid line is the best fit of the data, obtained by varying all parameters (Table 4), while the dash line is the fit of the data obtained by only varying R and t_f (Table 3), other parameter values being given by Table 2.

Table 4: **Estimated values of R , t_f , and physiological parameters, for groups G1 to G4.** Parameter values for group G0 are recalled for comparison purposes (in gray).

Group	R (d ⁻¹)	t_f (d)	C_α (d ⁻¹)	θ_α (cells.vol ⁻¹)	n_α (N.U)	C_σ (d ⁻¹)	RSS (N.U)
G0	5.0	3.0	20	$10^{6.5}$	11	0.7	6.0*
G1	8.0	0.6	55	$10^{6.2}$	24	0.7	2.1
G2	8.0	0.8	21	$10^{6.0}$	37	0.9	1.6
G3	0.5	2.0	4.5	$10^{6.2}$	2	0.7	0.9
G4	5.0	0.2	68	$10^{6.1}$	58	1.1	2.9

* This value may seem much higher than the other ones in the same column, but it has simply been computed using more experimental data (see Figure 4.B).

452 related to the apoptosis rate (C_α , θ_α , n_α) and to the self-renewal rate (C_σ)
 453 to vary, with the assumption that the self-renewal rate is constant. We
 454 then obtain the solid curves in Figure 11 and values given by Table 4. All
 455 results show a very good agreement of the simulation and the experimental
 456 measurements (see column ‘RSS’ in Table 4), variations of the hematocrit
 457 during the recovery phase (between day 3 and day 15 post-injection) are
 458 particularly well captured by the model. This stresses the ability of the
 459 model to describe stress erythropoiesis induced by various protocols of PHZ
 460 injections.

461 One may however notice that correct reproduction of the data is obtained
 462 for parameter values that are very different from one group to the other (see
 463 Table 4).

464 Regarding physiological rates, values of the self-renewal rate C_σ are con-
 465 sistent for all groups, with a doubling time between 7.5h and 12h. On the
 466 contrary, the apoptosis rate shows very different values of its three charac-
 467 teristic parameters among all groups. A careful investigation of the values
 468 of the apoptosis rate all along the response to PHZ injections first shows
 469 that for all groups the maximal value C_α is never reached. Second, contrary
 470 to what would be expected from the shape of the function α (see (5)), the
 471 apoptosis rate does not behave as a saturating function for groups G1, G2
 472 and G4, but rather as an exponential function (see Figure 12), with values
 473 ranging between 0 (when the number of erythrocytes is high, fully inhibiting
 474 progenitor apoptosis) and a maximum value in the interval $[3 \text{ d}^{-1}; 12 \text{ d}^{-1}]$,

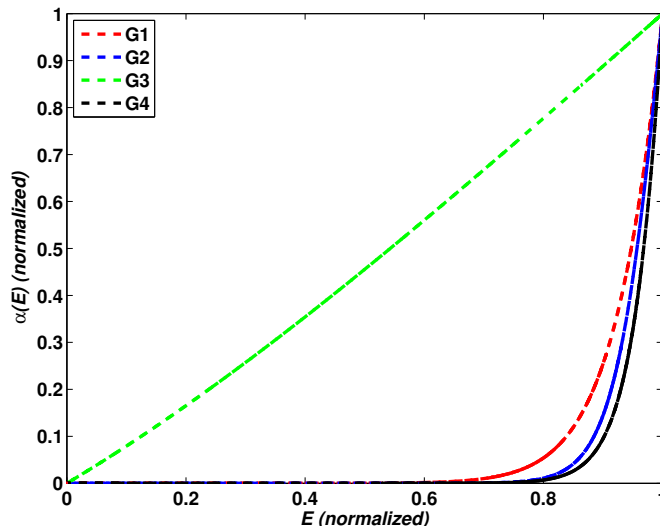


Figure 12: **Normalized values of $\alpha(E)$ over the anemia and the recovery phases, for groups G1 to G4.** On the x-axis, values of E taken during the simulation shown in Figure 11 have been normalized (0 represents the minimum value, 1 the maximum one). On the y-axis, corresponding values of $\alpha(E)$ have also been normalized.

475 far from the estimated maximum value C_α . For these groups, the estimated
 476 value of n_α is very high, hence the apoptosis function α is of threshold type.
 477 And since all estimated values of θ_α are larger than the steady state E^* , only
 478 the first increasing convex part of the function is actually used to regulate
 479 apoptosis, resulting in an exponential shape.

480 Group G3 displays very different features than the other groups: instead
 481 of an exponential behavior, the apoptosis rate appears to be almost linear
 482 (Figure 12). This comes from the estimated values of C_α and n_α , which are
 483 very low. Consequently the apoptosis rate α is linear far from the threshold
 484 value θ_α (on both sides of θ_α actually, even though only the left-hand side of
 485 θ_α is involved in the regulation in this case). Since the estimated value of θ_α
 486 is larger than the steady state value in group G3 as well, then we observe a
 487 linear regulation of the apoptosis rate. One can observe on Figure 11 that
 488 estimated recovery dynamics are different for group G3, compared to the
 489 other groups. They are characterized by a slower recovery and an absence of
 490 overshooting from the basal hematocrit value on the 4-8 days period. Since
 491 group G3 differs from the other ones – and particularly G1 and G2 – only

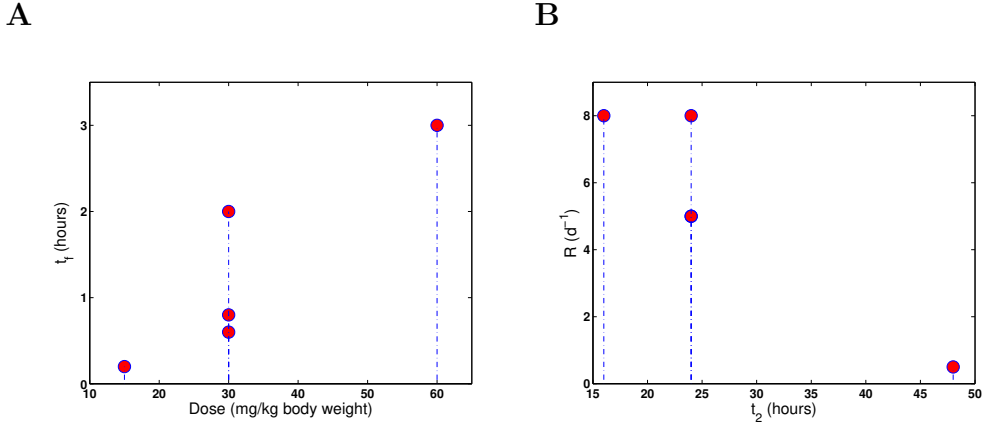


Figure 13: **Estimated values of t_f and R as functions of the dose and t_2 , respectively.** (A) Values of t_f for the three different doses (15, 30 and 60 mg/kg body weight). (B) Values of R for the three different t_2 values (0.7, 1 and 2 days). Values taken from Table 4.

492 by the time of the second injection (2 days after the initial injection), we
 493 may hypothesize that the 2-days period between PHZ injections allowed the
 494 organism to partly recover and in particular to perform a tighter control of
 495 erythroid progenitor death by apoptosis, that resulted in a slower recovery
 496 and a less strict regulation of Epo-mediated apoptosis.

497 Regarding values of parameters R and t_f , a trend appears on the way
 498 they are influenced by the dose or the time of second injection (Figure 13):
 499 the higher the dose the higher t_f , and to a lesser extent the sooner the second
 500 injection the higher R . Yet in each case a lot of variability is measured for
 501 groups with either the same dose or the same time of the second injection.
 502 Since R and t_f both are associated to the influence of PHZ on erythrocyte
 503 death, one parameter may compensate the influence of the other (R and t_f
 504 have been identified as key regulators of the value HCT_{min} in Section 3.2
 505 without clearly identifying their respective roles), resulting in the observed
 506 variability. In order to check that assumption, we drew the product $R \times t_f$
 507 (adimensionalized quantity) as a function of the dose and the second time of
 508 the injection (Figure 14). It clearly shows an influence of the experimental
 509 protocol in the estimated values of R and t_f : the higher the dose, the larger
 510 the product $R \times t_f$, and the sooner the second injection, the larger $R \times t_f$.
 511 This is particularly true when the dose (respectively, second injection time)

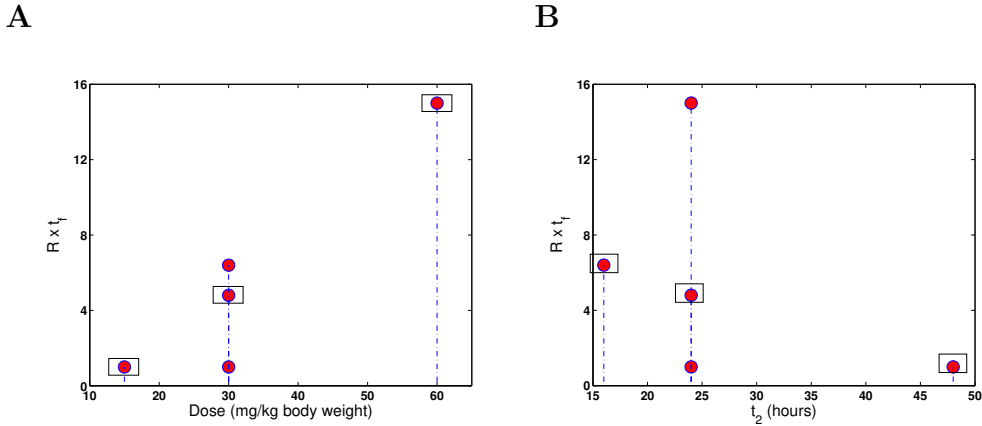


Figure 14: **Estimated values of $R \times t_f$ as function of the dose (A) and t_2 (B).** Within-boxes values share the same t_2 value (A) or dose (B). Values taken from Table 4.

512 effect is observed for a shared second injection time (respectively, dose): this
 513 is shown by squared dots in Figure 14, and the trend clearly appears.

514 Therefore, despite differences in parameter values between all groups, esti-
 515 mated values account for the various experimental protocols used to generate
 516 the data (groups G1 to G4) and the associated physiological responses. In
 517 addition, the influence of the experimental protocol clearly appears through
 518 the value of the product $R \times t_f$ that sums up the specifics of PHZ injections.

519 4. Discussion

520 We modified a previously published model of stress erythropoiesis in mice
 521 to explicitly describe and account for the specific phenylhydrazine-based way
 522 of inducing anemia experimentally. Contrary to bleeding-induced anemias for
 523 instance, phenylhydrazine-induced anemias not only reduce the quantity of
 524 red blood cells but also affect the entire red blood cell production process:
 525 indeed, phenylhydrazine either kills red blood cells – hence inducing an ane-
 526 mia – or damages red blood cell membranes and then shortens red blood cell
 527 lifespans with potential consequences on the organism behavior on the days
 528 following the anemia. Although the model cannot be solved analytically, we
 529 implemented an appropriate numerical method (Angulo et al., 2017) in order
 530 to numerically identify the respective influences of the experimental proto-
 531 col and physiological regulatory process on the model’s behavior. This gave

532 us insights into the way the organism deals with phenylhydrazine injections
533 inducing anemia and the recovery from the anemia.

534 First, our model proved its ability to reproduce experimental data con-
535 sisting in hematocrit measurements at several time points following phenyl-
536 hydrazine-induced anemia, with relevant estimated parameter values. We
537 showed that the strength of the anemia, induced by phenylhydrazine in-
538 jections, is mainly controlled by the experimental protocol (the quantity of
539 injected phenylhydrazine, the number of injections, and the time between
540 the two injections). The fall of the hematocrit observed in the days follow-
541 ing phenylhydrazine injections is strongly dependent upon three parameters,
542 R and t_f on one side, and t_2 on the other side, suggesting different roles
543 and targets of these parameters in the induction of the anemia. Parameter
544 t_2 characterizes the experimentalist's choice (the time at which the second
545 injection occurs) while R and t_f are mainly specific of phenylhydrazine's
546 properties (its strength in inducing death and how long its effects are felt by
547 the organism). On the contrary, we showed that the recovery phase is mainly
548 controlled by the regulation of physiological processes. Epo-mediated inhi-
549 bition of erythroid progenitor apoptosis, identified as the main regulator of
550 erythropoiesis for years (Koury and Bondurant, 1990), is a powerful mean
551 to speed up the recovery, because it can quickly adapt the production of
552 erythrocytes to strong modifications in circulating red blood cell counts.

553 Second, our model showed its ability to reproduce similar experimental
554 data, obtained with modified protocols: either the dose of phenylhydrazine
555 or the time of the second injection were modified in 4 different experiments,
556 and qualitatively similar yet quantitatively different dynamics were gener-
557 ated. Model simulations also managed to characterize each experimental
558 protocol by highlighting relationships between the injected dose or the time
559 of the second injection and an adimensionalized variable $R \times t_f$ that embeds
560 phenylhydrazine properties. This allows to directly link the experimental
561 protocol to the severeness of the anemia *via* the action of phenylhydrazine.
562 Consequently, respective influences of the experimental protocol and physi-
563 ological processes on the features of stress erythropoiesis can be separately
564 investigated. Moreover phenylhydrazine-induced anemias can be compared
565 even though the experimental protocol changes (different dose, different time
566 of the second injection), but can also be compared to other experimental pro-
567 tocols (for instance bleeding) thanks to the characterization of the protocol
568 by the combination of two variables, R and t_f .

569 Our description of the influence of phenylhydrazine on erythrocyte dy-

570 namics could be improved. Pharmacodynamics and pharmacokinetics of
571 phenylhydrazine could for instance be incorporated to the description of the
572 induction of the anemia, to directly relate features of the induced anemia
573 to phenylhydrazine properties, instead of indirect properties (residual effect,
574 etc.) as we did in this work. It is however difficult to properly define the PK-
575 PD of phenylhydrazine, as few information is accessible and so developing a
576 relevant PK-PD model of phenylhydrazine could represent an entire research
577 work.

578 Our study stresses the potential roles of additional processes: shorten-
579 ing or lengthening of differentiation times (characterized by τ_p in our model)
580 and increase or decrease of the stem cell flux from the hematopoietic stem
581 cell compartment could also strongly influence both the effect of phenylhy-
582 drazine on the organism and the recovery (Figures 8.B and 10). However,
583 to our knowledge, no experimental evidence ever showed that differentiation
584 times (or cell cycle durations) were modified during stress erythropoiesis.
585 Therefore, such a control of the organism's response to anemia remains hy-
586 pothetical at this stage. Regarding the influence of the differentiation of HSC
587 into erythroid progenitors, our results show that this could influence the re-
588 covery provided that large variations of the HSC flux are allowed, and that
589 these changes can occur on a very short time scale (almost instantaneously).
590 This is hardly the case, as HSC regulation is performed through several cell
591 cycles and important variations of the HSC population are not observed over
592 a short period of time in healthy individuals. These additional contributions
593 to the organism's response to anemia hence do not appear as relevant as the
594 regulation of erythroid progenitor apoptosis.

595 In Crauste et al. (2008), we concluded on the importance of accounting
596 for erythroid progenitor self-renewal when describing stress erythropoiesis,
597 and described a nonlinear erythrocyte-mediated regulation of self-renewal.
598 Our results confirm the relevance of accounting for erythroid progenitor self-
599 renewal, all parameter value estimation procedures leading to positive self-
600 renewal rates, whatever the experimental protocol. Nevertheless, our results
601 also indicate that regulation of the self-renewal rate is not necessary to ac-
602 count for appropriate dynamics: a constant self-renewal rate, corresponding
603 to a robust doubling time around 10h, allows to reproduce experimental dy-
604 namics. This can be explained by the nature of the apoptosis rate regulation:
605 erythroid progenitor apoptosis is highly regulated, and for normal red blood
606 cell counts estimations of the apoptosis rate are rather high (see Crauste et
607 al. (2008) for instance): in this case, a small population of self-renewing cells

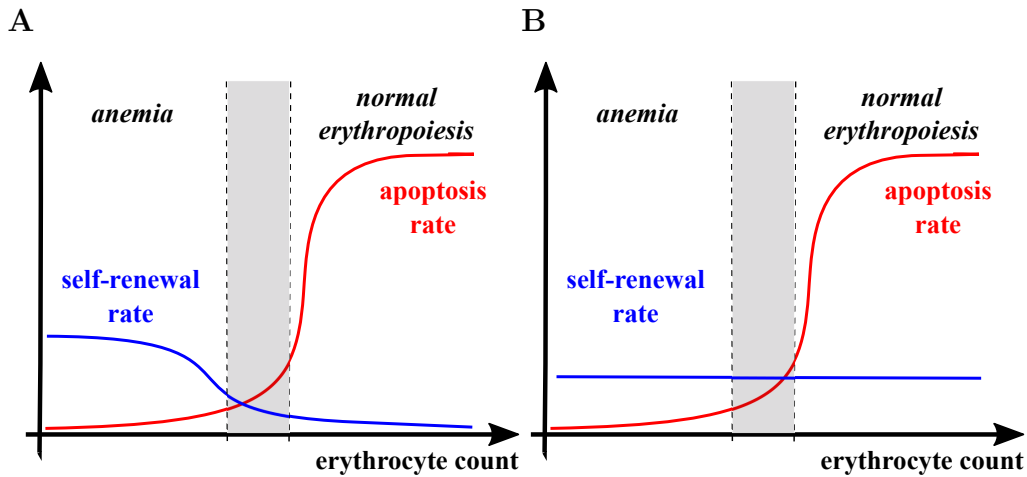


Figure 15: **Two scenarii for explaining regulatory process during stress erythropoiesis.** (A) The self-renewal rate depends on the erythrocyte count, see (5) (B) The self-renewal rate is constant. In both cases the apoptosis rate depends on the erythrocyte count, as in (5). Normal erythropoiesis corresponds to high erythrocyte counts, while anemia corresponds to low erythrocyte counts. The gray area corresponds to an unclear, a priori transient zone of low erythrocyte counts that does not necessitate a strong reaction from the organism.

608 among the progenitor population can hardly be detected. During stress ery-
 609 thropoiesis, and in particular during anemia, the strong regulation of apop-
 610 tosis can almost completely inhibit it, then making the self-renewal rate
 611 influential, without necessarily an opposite regulation (see Figure 15). Addi-
 612 tionally, this can lead to further analysis of the model, in particular system
 613 (1)-(4) can be mathematically analyzed when σ is constant whereas the anal-
 614 ysis has been impossible, to this day, for nonlinear self-renewal rates σ .

615 Regarding the erythroid progenitor apoptosis rate, our analysis showed
 616 that its regulation could be slightly different than the one we implemented
 617 in our model, that is a saturating function characterized by very low val-
 618 ues for small erythrocyte counts and very high values for high erythrocyte
 619 counts. As discussed in Section 3.6, values of the apoptosis rate measured
 620 through an entire simulation do not correspond to the spectrum that the
 621 saturating function could span: only the first increasing, convex part of this
 622 function is actually used to perform stress erythropoiesis. From a model-
 623 ing point of view, this indicates that instead of using a classical saturating
 624 Hill function to describe the erythrocyte count-dependent apoptosis rate, an

625 exponential increasing function could be used. This may not seem to rep-
626 resent an important contribution to erythropoiesis modeling, yet it would
627 allow describing the apoptosis rate using two parameters, instead of three
628 in the current version, hence favoring a better, more sensitive control of the
629 apoptosis regulation.

630 **Acknowledgements**

631 OA has been partially supported by project MTM2014-56022-C2-2-P of
632 the Spanish Ministerio de Economía y Competitividad and European FEDER
633 Funds. We thank Quentin Lamy for his technical help in collecting the data.
634 We thank Prof. Mark Koury for his support and for providing the bleeding-
635 induced anemia data in Figure 1.

636 A.S. Ackleh, H.T. Banks, K. Deng, A finite difference approximation for a
637 coupled system of nonlinear size-structured population, *Nonlinear Analysis*
638 50 (2002) 727–748, doi:10.1016/S0362-546X(01)00780-5

639 A.S. Ackleh, K. Deng, K. Ito, J. Thibodeaux, A structured erythropoiesis
640 model with nonlinear cell maturation velocity and hormone decay rate,
641 *Math. Bios.* 204 (2006) 21–48, doi:10.1016/j.mbs.2006.08.004.

642 A.S. Ackleh, J. Thibodeaux, Parameter Estimation in a Structured Erythro-
643 poiesis Model. *Math. Bios. Eng.* 5 (2008) 601-616.

644 M. Adimy, F. Crauste, S. Ruan, Modelling hematopoiesis mediated by growth
645 factors with applications to periodic hematological diseases. *Bull. Math.*
646 *Biol.* 68 (8) (2006) 2321–2351.

647 O. Angulo, F. Crauste, J.C. López-Marcos, Numerical integration
648 of an erythropoiesis model with explicit growth factor dynam-
649 ics, *Journal of Computational and Applied Mathematics* (2017)
650 <https://doi.org/10.1016/j.cam.2017.01.033>.

651 O. Angulo, J.C. López-Marcos, M.A. Bees, Mass Structured Systems with
652 Boundary Delay: Oscillations and the Effect of Selective Predation, *J.*
653 *Nonlinear Sci.* 22 (2012) 961–984.

654 O. Angulo, J.C. López-Marcos, M.A. López-Marcos, Numerical approxima-
655 tion of singular asymptotic states for a size-structured population model
656 with a dynamical resource, *Math. Comput. Model.* 54 (2011a) 1693–1698.

- 657 O. Angulo, J.C. López-Marcos, M.A. López-Marcos, A semi-Lagrangian
658 method for a cell population model in a dynamical environment *Math.*
659 *Comput. Model.* 57 (2013a) 1860–1866.
- 660 O. Angulo, J.C. López-Marcos, M.A. López-Marcos, J. Martínez-Rodríguez,
661 Numerical investigation of the recruitment process in open marine pop-
662 ulation models, *J. Stat. Mech.*, (2011b) P01003 doi: 10.1088/1742-
663 5468/2011/01/P01003.
- 664 O. Angulo, J.C. López-Marcos, M.A. López-Marcos, J. Martínez-Rodríguez,
665 Numerical analysis of a population model of marine invertebrates with
666 different life stages, *Commun. Nonlinear Sci. Numer. Simul.* 18 (2013b)
667 2153–2163.
- 668 H.T. Banks, C.E. Cole, P.M. Schlosser, T. Hien, Modelling and Optimal
669 Regulation of Erythropoiesis Subject to Benzene Intoxication, *Math. Bio.*
670 *Engineering* 1 (1) (2004) 15–48.
- 671 A. Bauer, F. Tronche, O. Wessely, C. Kellendonk, H.M. Reichardt, P. Stein-
672 lein, G. Schutz, H. Beug, The glucocorticoid receptor is required for stress
673 erythropoiesis, *Genes Dev.* 13 (1999) 2996–3002.
- 674 J. Bélair, M.C. Mackey, J.M. Mahaffy, Age-structured and two-delay models
675 for erythropoiesis, *Math. Biosci.* 128 (1995) 317–346, doi:10.1016/0025-
676 5564(94)00078-E.
- 677 N.I. Berlin, C. Lotz, Life span of the red blood cell of the rat following acute
678 hemorrhage, *Proc. Soc. Exp. Biol. Med.* 78 (1951) 788.
- 679 F. Crauste, L. Pujon-Menjouet, S. Génieys, C. Molina, O. Gandrillon, Adding
680 self-renewal in committed erythroid progenitors improves the biological
681 relevance of a mathematical model of erythropoiesis, *J. Theor. Biol.* 250
682 (2008) 322–338.
- 683 N. Eymard, N. Bessonov, O. Gandrillon, M.J. Koury, V. Volpert, The role
684 of spatial organization of cells in erythropoiesis, *J Math Biol.* 70 (2015)
685 71–97.
- 686 O. Gandrillon, U. Schmidt, H. Beug, J. Samarut, TGF-beta cooperates with
687 TGF-alpha to induce the self-renewal of normal erythrocytic progenitors:
688 evidence for an autocrine mechanism, *Embo. J.* 18 (1999) 2764–2781.

- 689 M.J. Koury, M.C. Bondurant, Erythropoietin retards DNA breakdown and
690 prevents programmed death in erythroid progenitor cells, *Science* 248
691 (1990) 378–381.
- 692 M. Loeffler, H.E. Wichmann, A comprehensive mathematical model of stem
693 cell proliferation which reproduces most of the published experimental re-
694 sults, *Cell Tissue Kinet.* 13 (1980) 543–561.
- 695 M. Loeffler, K. Pantel, H. Wulff, H.E. Wichmann, A mathematical model of
696 erythropoiesis in mice and rats. Part 1. Structure of the model, *Cell Tissue*
697 *Kinet.* 22 (1989) 3–30.
- 698 M.C. Mackey, Unified hypothesis of the origin of aplastic anaemia and peri-
699 odic hematopoiesis, *Blood* 51 (1978) 941–956.
- 700 J.M. Mahaffy, J. Belair, M.C. Mackey, Hematopoietic model with moving
701 boundary condition and state dependent delay: applications in erythro-
702 poiesis, *J. Theor. Biol.* 190 (1998) 135–146, doi:10.1006/jtbi.1997.0537.
- 703 K. Nagai, K. Oue, H. Kawagoe, Studies on the short-lived reticulocytes by
704 use of the in vitro labeling method, *Acta Haematol. Jpn* 31 (1968) 967.
- 705 K. Nagai, K. Ishizu, E. Kakishita, Studies on the erythroblast dynamics
706 based on the production of fetal hemoglobin, *Acta Haematol. Jpn* 34
707 (1971).
- 708 B. Pain, C.M. Woods, J. Saez, T. Flickinger, M. Raines, H.J. Kung, S.
709 Peyrol, C. Moscovici, G. Moscovici, P. Jurdic, E. Lazarides, J. Samarut,
710 EGF-R as a hemopoietic growth factor receptor: The c-erbB product is
711 present in normal chicken erythrocytic progenitor cells and controls their
712 self-renewal, *Cell* 65 (1991) 37–46, doi:10.1016/0092-8674(91)90405-N.
- 713 L. Pujo-Menjouet, S. Bernard, M.C. Mackey, Long period oscillations in a
714 G_0 model of hematopoietic stem cells, *SIAM J. Appl. Dynam. Syst.* 4 (2)
715 (2005) 312–332.
- 716 L. Pujo-Menjouet, M.C. Mackey, Contribution to the study of periodic
717 chronic myelogenous leukemia, *C. R. Biologies* 327 (2004) 235–244,
718 doi:10.1016/j.crvi.2003.05.004.

- 719 A. Raue, C. Kreutz, T. Maiwald, J. Bachmann, M. Schilling, U. Klingmüller,
720 J. Timmer, Structural and practical identifiability analysis of partially ob-
721 served dynamical models by exploiting the profile likelihood, *Bioinformat-*
722 *ics* 25 (2009) 1923–1929.
- 723 M.M. Rhodes, S.T. Koury, P. Kopsombut, C.E. Alford, J.O. Price, M.J.
724 Koury, Stress reticulocytes lose transferrin receptors by an extrinsic process
725 involving spleen and macrophages, *Am J Hematol.* 91 (2016) 875–882.
- 726 I. Roeder, Quantitative stem cell biology: computational studies in the
727 hematopoietic system, *Curr. Opin. Hematol.* 13 (2006) 222–228.
- 728 I. Roeder, M. Loeffler, A novel dynamic model of hematopoietic stem cell or-
729 ganization based on the concept of within-tissue plasticity, *Exp. Hematol.*
730 30 (2002) 853–861.
- 731 A. Shimada, The maturation of reticulocytes. II. Life-span of red cells orig-
732 inating from stress reticulocytes, *Acta Med. Okayama* 29 (4) (1975) 283–
733 289.
- 734 F. Stohlman, Humoral regulation of erythropoiesis. VII. Shortened survival
735 of erythrocytes by erythropoietin or severe anemia, *Proc. Soc. Exp. Biol.*
736 *Med.* 107 (1961) 884.
- 737 H. Walter, E.J. Krob, G.S. Ascher, Abnormal membrane surface properties
738 during maturation of rat reticulocytes elicited by bleeding as measured by
739 partition in two-polymer aqueous phases, *Br. J. Haematol.* 31 (2) (1975)
740 149–157.
- 741 F.M. Watt, B.L. Hogan, Out of Eden: stem cells and their niches. *Science*
742 287 (2000) 1427–1430.
- 743 G. Webb, Theory of nonlinear age-dependent population dynamics, Mono-
744 graphs and textbooks in Pure and Appl. Math., vol 89, Marcel Dekker,
745 New York, 1985.
- 746 H.E. Wichman, M. Loeffler, *Mathematical Modeling of Cell Proliferation*,
747 CRC, Boca Raton, FL, 1985.
- 748 H.E. Wichman, M. Loeffler, S. Schmitz, A concept of hemopoietic regulation
749 and its biomathematical realisation, *Blood Cells* 14 (1985) 411–429.

750 H.E. Wichman, M. Loeffler, K. Pantel, H. Wulff, A mathematical model of
751 erythropoiesis in mice and rats. Part 2. Stimulated erythropoiesis, Cell
752 Tissue Kinet. 22 (1989) 31–49.